To the Graduate Council:

I am submitting herewith a thesis written by Walter L. Trammell entitled "Comparison of the Fresnel Approximation Method and the Exact Method for the Determination of the E-field of an E-plane Sectoral Horn." I have examined the final copy of this thesis for form and content and recommend that it be accepted in partial fulfillment of the requirements for the degree of Master of Science, with a major in Electrical Engineering.

James D. Tillman
James D. Tillman
Major Professor

We have read this thesis
and recommend its acceptance:

Herbert S. Ruff Jr.

R. W. Hoffman

Accepted for the Council:

Vice Provost
and Dean of The Graduate School

COMPARISON OF THE FRESNEL APPROXIMATION METHOD AND THE EXACT METHOD FOR THE DETERMINATION OF THE E-FIELD OF AN E-PLANE SECTORAL HORN

A Thesis

Presented for the

Master of Science

Degree

The University of Tennessee, Knoxville

Walter L. Trammell

May 1989

ACKNOWLEDGMENTS

In the research and assembly of this thesis, four individuals have helped me considerably with their consultation. I am indebted to Dr. J.D. Tillman, Dr. H.P. Neff, Dr. G.W. Hoffman, and L.A. Bugos for their help and support. Thank you gentlemen.

ABSTRACT

Horn antennas play a vital role in modern microwave communication systems. An accurate determination of their fields is essential to the design and implementation of these antennas. A simple and reliabale method to determine these fields is needed.

Two methods for the calculation of the electric fields of an E-plane sectoral horn are discussed in this thesis. The exact method uses the asymptotic approximation of the Hankel function to calculate the field and pattern. The asymptotic approximations are used whenever possible due to the large amount of computer time involved when evaluating Hankel functions.

The Fresnel approximation method uses the sine and cosine Fresnel integrals and divides the horn into one, two, or three sections. The field is found for each of these sections and then combined for a more accurate approximation. The major problem associated with the Fresnel approximation is the phase error. When a wave travels down the length of the horn, different parts of the wave reach the aperture at different times. The result is phase error. By dividing the horn into two or three sections, the phase error is reduced and the electric field approximated more accurately.

The Fresnel approximation was found to approach the exact method as the flare angle of the horn decreased. However, the calculation of the field by the Fresnel approximation required more computer time than for the exact method.

Although the broadness of the patterns for both methods matched closely, the exact method failed to show the lobes of these patterns. This results from the horn being of finite length. In the derivation of the exact method, the sides of the horn are assumed to extend to infinity.

From this evaluation, it is obvious that each method has its advantages. The Fresnel approximation consumes more computer time, but gives an accurate projection of the lobes. The exact method gives a good general shape of the pattern and takes less computer time, but does not give a good description of the lobes.

TABLE OF CONTENTS

LIST OF TABLES

LIST OF FIGURES

CHAPTER I

FRESNEL APPROXIMATION DERIVATION

We will first derive the Fresnel approximation for the electric field for an E-plane sectoral horn [1]. In our horn, the fields of the feed waveguide are of the dominant TE_{10} mode and the horn length is large compared to the dimensions of the aperture. The lowers order mode fields at the aperture of the horn are given by

$$E_z' = E_x' = 0 \tag{1.1}$$

and

$$E_y'(x', y') \simeq E_1 \cos(\pi x'/a)\, e^{-j[k y'^2/(2\rho_1)]} \tag{1.2}$$

where

$$\rho_1 = \rho_2 \cos\Psi_e \tag{1.3}$$

and E_1 is a constant.

The fields at the aperture are denoted by primes. The E-plane sectoral horn and the coordinate system are given in Figure 1.1.

In our horn, the waves radiate outward cylindrically from x. When the wavefront reaches the aperture at x', it has not reached the aperture at any other point. We denote this phase lag by $\delta(y)$.

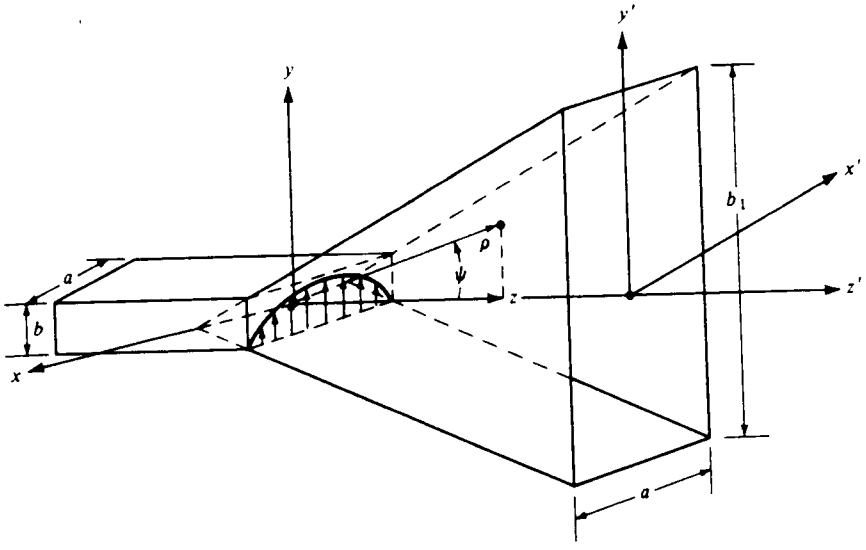

(a) *E*-plane horn

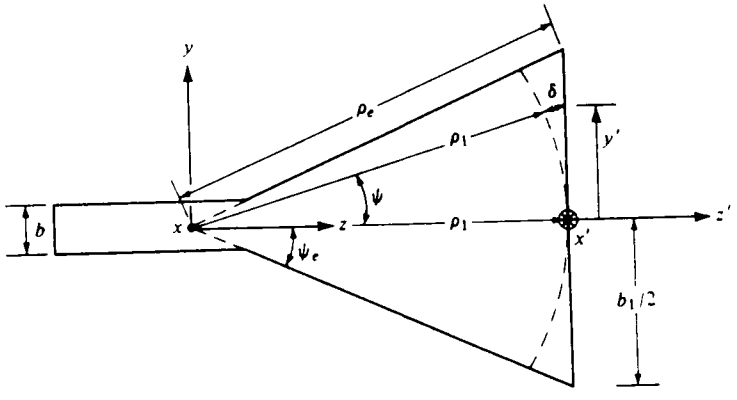

(b) *E*-plane view

Figure 1.1. The E-plane horn and coordinate system

The phase lag can be found for any point y' by

$$\left[\rho_1 + \delta(y')\right]^2 = \rho_1^2 + (y')^2, \tag{1.4}$$

which yields the expression

$$\delta(y') = -\rho_1 + \rho_1\left[1 + \left(\frac{y'}{\rho_1}\right)^2\right]^{1/2}. \tag{1.5}$$

$\delta(y')$ is now expanded binomially and the first two terms are retained. $\delta(y')$ reduces to

$$\delta(y') \simeq -\rho_1 + \rho_1\left[1 + \frac{1}{2}\left(\frac{y'}{\rho_1}\right)^2\right] = \frac{1}{2}\left(\frac{(y')^2}{\rho_1}\right). \tag{1.6}$$

The θ and the ϕ components are given in our spherical coordinate system by

$$N\theta = \iint_S \left[J_x \cos\theta\cos\phi + J_y \cos\theta\sin\phi - J_z \sin\theta\right] e^{jkr'\cos\Psi} ds', \tag{1.7}$$

$$N\phi = \iint_S \left[-J_x \sin\phi + J_y \cos\phi\right] e^{jkr'\cos\Psi} ds', \tag{1.8}$$

$$L\theta = \iint_S \left[M_x \cos\theta\cos\phi + M_y \cos\theta\cos\phi - M_z \sin\theta\right] e^{jkr'\cos\Psi} ds', \tag{1.9}$$

$$L\phi = \iint \left[-M_x \sin\phi + M_y \cos\phi\right] e^{jkr'\cos\Psi} ds'. \tag{1.10}$$

The E_r, E_θ, and E_ϕ fields are determined by

$$E_r = 0 \quad , \tag{1.11}$$

$$E_\theta = \frac{-jke^{-jkr}}{4\pi r}\left(L_\phi + \eta N_\theta\right) \quad , \tag{1.12}$$

and

$$E_\phi = \frac{jke^{-jkr}}{4\pi r}\left(L_\theta - \eta N_\phi\right) . \tag{1.13}$$

When the horn is not mounted on an infinite ground plane, the field distribution is given by

$$\left.\begin{aligned} E_a &= \hat{a}_y E_o \\ H_a &= -\hat{a}_y E_o/\eta \end{aligned}\right\} \quad \begin{aligned} &-a/2 \le x' \le a/2 \\ &-b/2 \le y' \le b/2 \quad , \end{aligned} \tag{1.14}$$

where Eo is a constant.

A closed surface is chosen that covers the entire x-y plane and Jy and Mx are formed over this surface. This gives us

$$\left.\begin{aligned} J_y &= -\frac{E_i}{\eta}\cos\left(\frac{\pi x'}{a}\right)e^{-jk\delta(y')} \\ M_x &= E_i \cos\left(\frac{\pi x'}{a}\right)e^{-jk\delta(y')} \end{aligned}\right\} \quad \begin{aligned} &-a/2 \le x' \le a/2 \\ &-b/2 \le y' \le b/2 \end{aligned} \tag{1.15}$$

and Mx and Jy = 0 elsewhere. (1.16)

From equation (1.7), we obtain

$$N_\phi = \frac{E_1}{\eta} \cos\theta \sin\phi \, I_1 I_2 . \tag{1.17}$$

I_1 and I_2 are given by

$$I_1 = \int_{-a/2}^{a/2} \cos\left(\frac{\pi x'}{a}\right) e^{-jkx \sin\theta\cos\phi} \, dx' \tag{1.18}$$

and

$$I_2 = \int_{-b/2}^{b/2} e^{-jk[\delta(y') - y'\sin\theta\cos\phi]} \, dy'. \tag{1.19}$$

I_1 can be written as

$$I_1 = -\left(\frac{\pi a}{2}\right)\left[\frac{\cos\left(\frac{ka}{2}\sin\theta\cos\phi\right)}{\left(\frac{ka}{2}\sin\theta\cos\phi\right)^2 - \left(\frac{\pi}{2}\right)^2}\right]. \tag{1.20}$$

I_2 can be written as

$$I_2 = \sqrt{\frac{\pi\rho_1}{k}} e^{j(k_y^2\rho_1/2k)}\left[C(t_2) - C(t_1)\right] - j\left[S(t_2) - S(t_1)\right], \tag{1.21}$$

where

$$t_1 = \sqrt{\frac{1}{\pi k \rho_1}}\left[-\frac{kb_1}{2} - k_y\rho_1\right], \tag{1.22}$$

$$t_2 = \sqrt{\frac{1}{\pi k \rho_1}} \left[\frac{k b_1}{2} - k_y \rho_1 \right] , \tag{1.23}$$

$$C(x) = \int_0^x \cos\left(\frac{\pi}{2} t^2\right) dt , \tag{1.24}$$

$$S(x) = \int_0^x \sin\left(\frac{\pi}{2} t^2\right) dt , \tag{1.25}$$

and

$$k_y = k \sin\theta \sin\phi . \tag{1.26}$$

Using (1.20) and (1.21), we can write (1.17) as

$$N_\theta = \frac{E_1 \pi a}{2} \sqrt{\frac{\pi \rho_1}{k}} \; e^{j(k_y^2 \rho_1 / 2k)}$$

$$\cdot \left[\frac{\cos\theta \sin\phi}{\eta} \left[\frac{\cos\left(\frac{k_x a}{2}\right)}{\left(\frac{k_x a}{2}\right)^2 - \left(\frac{\pi}{2}\right)^2} \right] F(t_1, t_2) \right] , \tag{1.27}$$

where

$$k_x = k \sin\theta \cos\phi , \tag{1.28}$$

$$k_y = k \sin\theta \sin\phi, \tag{1.29}$$

and

$$F(t_1, t_2) = [C(t_2) - C(t_1)] - j[S(t_2) - S(t_1)]. \tag{1.30}$$

N_ϕ in (1.9) can be written as

$$N_\phi = \frac{E_1 \pi a}{2} \sqrt{\frac{\pi \rho_1}{k}}\, e^{j(k_y^2 \rho_1 / 2k)} \cdot \left[\frac{\cos\phi}{\eta} \left[\frac{\cos\left(\frac{k_x a}{2}\right)}{\left(\frac{k_x a}{2}\right)^2 - \left(\frac{\pi}{2}\right)^2} \right] F(t_1, t_2) \right]. \tag{1.31}$$

L_θ in (1.10) can be written as

$$L_\theta = \frac{E_1 \pi a}{2} \sqrt{\frac{\pi \rho_1}{2}}\, e^{j(k_y^2 \rho_1 / 2k)} \cdot \left[-\cos\theta \cos\phi \left[\frac{\cos\left(\frac{k_x a}{2}\right)}{\left(\frac{k_x a}{2}\right)^2 - \left(\frac{\pi}{2}\right)^2} \right] F(t_1, t_2) \right]. \tag{1.32}$$

L_ϕ in (1.11) can be written as

$$L_\phi = \frac{E_1 \pi a}{2} \sqrt{\frac{\pi \rho_1}{2}}\, e^{j(k_y^2 \rho_1 / 2k)}$$

$$\cdot \left[\sin\phi \left[\frac{\cos\left(\frac{k_x a}{2}\right)}{\left(\frac{k_x a}{2}\right)^2 - \left(\frac{\pi}{2}\right)^2} \right] F(t_1, t_2) \right] . \tag{1.33}$$

Using (1.12), (1.13) and (1.27)-(1.33), the electric field components of the horn can be written as

$$E_r = 0 \quad , \tag{1.34}$$

$$E_\theta = \frac{-ja\sqrt{\pi k \rho_1}}{8r}\, E_1\, e^{-jkr} \left[e^{j(k_y^2 \rho_1 / 2k)} \sin\phi (1 + \cos\theta) \right]$$

$$\cdot \left[\frac{\cos\left(\frac{k_x a}{2}\right)}{\left(\frac{k_x a}{2}\right)^2 - \left(\frac{\pi}{2}\right)^2} \right] F(t_1, t_2), \tag{1.35}$$

and

$$E_\phi = \frac{-ja\sqrt{\pi k \rho_1}}{8r} E_1 e^{-jkr} \left[e^{j(k_y^2 \rho_1 / 2K)} \sin\phi \, (1+\cos\theta) \right]$$

$$\cdot \left[\frac{\cos\left(\frac{k_x a}{2}\right)}{\left(\frac{k_x a}{2}\right)^2 - \left(\frac{\pi}{2}\right)^2} \right] F(t_1, t_2) \, . \qquad (1.36)$$

In the E-plane, where $\phi = \pi/2$, the electric field reduces to

$$E_r = E_\phi = 0 \qquad (1.37)$$

and

$$E_\theta = \frac{-ja\sqrt{\pi k \rho_1}}{8r} E_1 \, e^{-jkr}$$

$$\cdot \left[- e^{j(k\rho_1 \sin^2\theta/2)} \left(\frac{2}{\pi}\right)^2 (1+\cos\theta) F(t_1', t_2') \right] , \qquad (1.38)$$

where

$$F(t_1', t_2') = [C(t_2') - C(t_1')] - j[S(t_2') - S(t_1')] \, , \qquad (1.39)$$

$$t_1' = \sqrt{\frac{k}{\pi \rho_1}} \left(- \frac{b_1}{2} - \rho_1 \sin\theta \right) , \qquad (1.40)$$

$$t_2' = \sqrt{\frac{k}{\pi \rho_1}}\left(+\frac{b_1}{2} - \rho_1 \sin\theta\right). \tag{1.41}$$

The absolute value of E_θ becomes

$$|E_\theta| = \frac{a\sqrt{2\rho_1}}{2\pi r}(1+\cos\theta)\left|F(t_1', t_2')\right|. \tag{1.42}$$

The calculation of E_θ is given in PROGRAM ONE.

In the H-plane, where $\phi=0$, the electric field reduces to

$$E_r = E_\theta = 0 \tag{1.43}$$

and

$$E_\phi = -\frac{ja\sqrt{\pi k \rho_1}}{8r} E_1^{-jkr}$$

$$\cdot\left[(1+\cos\theta)\left[\frac{\cos\left(\frac{ka}{2}\sin\theta\right)}{\left(\frac{ka}{2}\sin\theta\right)^2-\left(\frac{\pi}{2}\right)^2}\right]F(t_1'', t_2'')\right], \tag{1.44}$$

where

$$F(t_1'', t_2'') = [C(t_2'') - C(t_1'')] - j[S(t_1'') - S(t_2'')], \tag{1.45}$$

$$\gamma_1'' = \frac{-b_1}{2}\sqrt{\frac{k}{\pi\rho_1}} \quad , \tag{1.46}$$

and

$$\gamma_2'' = \frac{b_1}{2}\sqrt{\frac{k}{\pi\rho_1}} \quad . \tag{1.47}$$

The absolute value of $E\phi$ becomes

$$|E\phi| = \frac{a}{8r}\sqrt{2\pi^2\rho_1}\,(1+\cos\theta)$$

$$\cdot\left[\frac{\cos\left(\frac{ka}{2}\sin\theta\right)}{\left(\frac{ka}{2}\sin\theta\right)^2-\left(\frac{\pi}{2}\right)^2}\right]\left|F(\gamma_1'', \gamma_2'')\right| \quad . \tag{1.48}$$

The calculation of $|E\phi|$ is given in PROGRAM TWO.

CHAPTER II

DERIVATION OF THE EXACT SOLUTION

We will begin our derivation of the exact solution for the E-field in our E-plane sectoral horn with Maxwell's equations in cylindrical form [2].

$$j\omega\epsilon\rho E_y = \frac{\partial}{\partial\rho}(\rho H_\rho) - \frac{\partial}{\partial\phi} H_\rho, \tag{2.1}$$

$$j\omega\epsilon\rho E_\rho \frac{\partial}{\partial\phi} H_y - \frac{\partial}{\partial y}(\rho H_\rho), \tag{2.2}$$

$$j\omega\epsilon E_\phi = \frac{\partial}{\partial y} H_\rho - \frac{\partial}{\partial\rho} H_y, \tag{2.3}$$

$$-j\omega\mu\rho H_y = \frac{\partial}{\partial\rho}(\rho E_\phi) - \frac{\partial}{\partial\phi} E_\rho, \tag{2.4}$$

$$-j\omega\mu\rho H_\rho = \frac{\partial}{\partial\rho} E_y - \frac{\partial}{\partial y}(\rho E_\phi), \tag{2.5}$$

$$j\omega\mu H_\phi = \frac{\partial}{\partial y} E_\rho - \frac{\partial}{\partial\rho} E_y. \tag{2.6}$$

For the Hom wave we are interested in, E_ρ, E_ϕ, and H_4 are zero. Maxwell's equations reduce to

$$j\omega\epsilon\rho E_4 = \frac{\partial}{\partial\rho}\left(\rho H_\phi\right) - \frac{\partial}{\partial\phi} H_\rho \,, \tag{2.7}$$

$$-j\omega\mu\rho H_\rho = \frac{\partial}{\partial\phi} E_4 \,, \tag{2.8}$$

and

$$j\omega\mu H_\phi = \frac{\partial}{\partial\rho} E_4 . \tag{2.9}$$

Now we solve for Ey in (2.8) and (2.9) and put them into (2.7) to obtain

$$\left[\frac{\partial^2}{\partial\rho^2} + \frac{1}{\rho}\frac{\partial}{\partial\rho} + \frac{1}{\rho^2}\frac{\partial^2}{\partial\phi^2} + \left(\frac{\omega}{c}\right)^2\right] E_4 = 0 . \tag{2.10}$$

This equation has a general solution of the form

$$E_4 = \left[A\sin(mv\phi) + B\cos(mv\phi)\right]\left[CJmv\left(\frac{\omega\rho}{c}\right) + DYmv\left(\frac{\omega\rho}{c}\right)\right], \tag{2.11}$$

where A,B,C, and D are complex constants and Jmv and Ymv are Bessel functions of the first and second kind and of the mvth order.

In our horn, only the Hom waves with an electric field of even symmetry radiate beams with a central lobe. Therefore it is only necessary to retain the cosine term in our solution.

The wave that is propagated in the radial direction can be represented by a Hankel function such that

$$K_{mv} = J_{mv} - j\,Y_{mv}. \tag{2.12}$$

From this, we determine

$$C = 1 \qquad \text{and} \tag{2.13}$$

$$D = -j. \tag{2.14}$$

Our solution now becomes

$$E_y = B\cos(mv\phi)\,K_{mv}\left(\frac{2\pi\rho}{\lambda}\right). \tag{2.15}$$

We now impose the boundary conditions to solve for the constant mv. Since there is no electric field in our wave that is tangential to the top and bottom surfaces of the horn, the boundary conditions are satisfied for y=(0,a). The horn with these boundaries is given in Figure 2.1.

$$\text{At the side, where } \phi = \pm \phi_o/2, \tag{2.16}$$

$$\text{Ey must go to zero. This gives us } \cos(mv\phi_o/2) = 0, \tag{2.17}$$

$$\text{which is satisfied by letting } mv = m\pi/\phi_o. \tag{2.18}$$

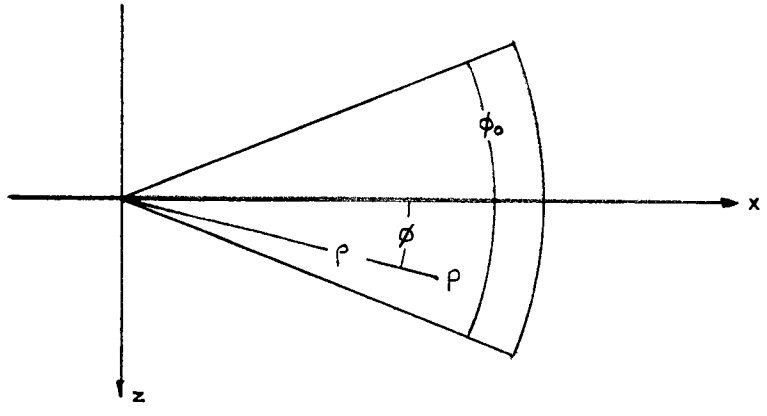

Figure 2.1. E-plane horn used for exact derivation.

where m=1, for the preferred H_{01} wave.

Our solution for Ey now becomes

$$E_y = B\cos(\pi\phi/\phi_0)\, K_{\pi/\phi_0}(2\pi\rho/\lambda). \tag{2.19}$$

When ρ is large, B can be approximated as

$$B = 2\pi/\lambda. \tag{2.20}$$

K_{π/ϕ_0} can be approximated as

$$K_{\pi/\phi_0} = \sqrt{\frac{2\lambda}{2\pi^2\rho}}\, e^{j[2\pi(\rho/\lambda) - ((2\pi/\phi_0 - 1)/4)\pi]}. \tag{2.21}$$

Using these approximations, our solution reduces to

$$E_y = 2\pi\cos(\pi\phi/\phi_0)\sqrt{\frac{2}{2\pi^2\rho}}\, e^{j[2\pi\rho - ((2\pi/\phi_0 - 1)/4)\pi]}. \tag{2.22}$$

Ey is now resolved into spherical coordinates and its absolute value is found. The result is $|E_\theta|$, which is given by

$$|E_\theta| = 2\pi\cos(\pi\phi/\phi_0)\sqrt{\frac{2}{2\pi^2\rho}}. \tag{2.23}$$

The calculation of $|E_\theta|$ for the inside of an E-plane horn is given by PROGRAM THREE.

In our derivation of the E_ϕ field, we know that Ey and E_ρ equal zero. This reduces our Maxwell's equations group to

$$-j\omega\epsilon E_\phi = \frac{\partial}{\partial y} H_\rho - \frac{\partial}{\partial \rho} H_y, \tag{2.24}$$

$$j\omega\mu\rho H_y = -\frac{\partial}{\partial\rho}(\rho E_\phi) , \tag{2.25}$$

and

$$j\omega\mu\rho H_\rho = \frac{\partial}{\partial y}(\rho E_\phi) . \tag{2.26}$$

We solve for Hy and H_ρ in (2.25) and (2.26) and put these into (2.24) to get

$$\left[\frac{\partial^2}{\partial\rho^2} + \frac{1}{\rho}\frac{\partial}{\partial\rho} + \left(\frac{\omega}{c}\right)^2 + \frac{\partial}{\partial y^2} - \frac{1}{\rho}\right] E_\phi = 0 . \tag{2.27}$$

This equation has a solution of the form

$$E_\phi = B\begin{matrix}\sin\\\cos\end{matrix}(\gamma y) K_1\left[\left(\sqrt{\left(\frac{\omega}{c}\right)^2 - \gamma^2}\right)\rho\right] . \tag{2.28}$$

Our boundary conditions require that E_ϕ vanish at y=(0,a). For y=0, the cosine term vanishes. At y=a,

$$\sin\gamma y = 0. \tag{2.29}$$

We solve for γ and obtain

$$\gamma = n\pi/a , \tag{2.30}$$

where n=1.

Our solution reduces to

$$E_\phi = B\sin\left(\frac{\pi y}{a}\right) K_1\left[\left(\sqrt{\left(\frac{\omega}{c}\right)^2 - \left(\frac{\pi}{a}\right)^2}\right)\rho\right] . \tag{2.31}$$

In our solution, we will look at the field on axis in the center of the aperture, where y=a/2. At y=a/2,

$$\sin\left(\frac{\pi y}{a}\right) = 1 \,. \tag{2.32}$$

Our solution now becomes

$$E_\phi = B K_1\left[\left(\sqrt{\left(\frac{2\pi}{\rho}\right)^2-\left(\frac{\pi}{a}\right)^2}\right)\rho\right]. \tag{2.33}$$

Using the asymptotic expression for the Hankel function with large ρ , and the value for the constant B , we can approximate E_ϕ as

$$E_\phi = \sqrt{(2\pi/\lambda)^2-(\pi/a)^2}\sqrt{\frac{2\lambda}{2\pi^2\rho}}\; e^{-j[2\pi\rho-((2\phi/\phi_o-1)/4)\pi]}. \tag{2.34}$$

Taking the absolute value of E_ϕ , we have

$$|E_\phi| = \sqrt{(2\pi/\lambda)^2-(\pi/a)^2}\sqrt{\frac{2\lambda}{2\pi^2\rho}}\,. \tag{2.35}$$

The calculation of $|E_\phi|$ for the inside of an E-plane sectoral horn is given in PROGRAM FOUR.

The radiation patterns and the field strengths outside the horn can be found by means of Huygens principle. The coordinate system we use to find these is given in Figure 2.3.

The radiation field is obtained from the Hertzian vector II. Using this, E is given by

$$E = (2\pi)^2 \Pi + \text{grad div}\,\Pi \,. \tag{2.36}$$

If we let divII=0. Ey is given by

$$j_4 \Pi_4 = j_4\left(\frac{1}{2\pi}\right)^2 E_4 \tag{2.37}$$

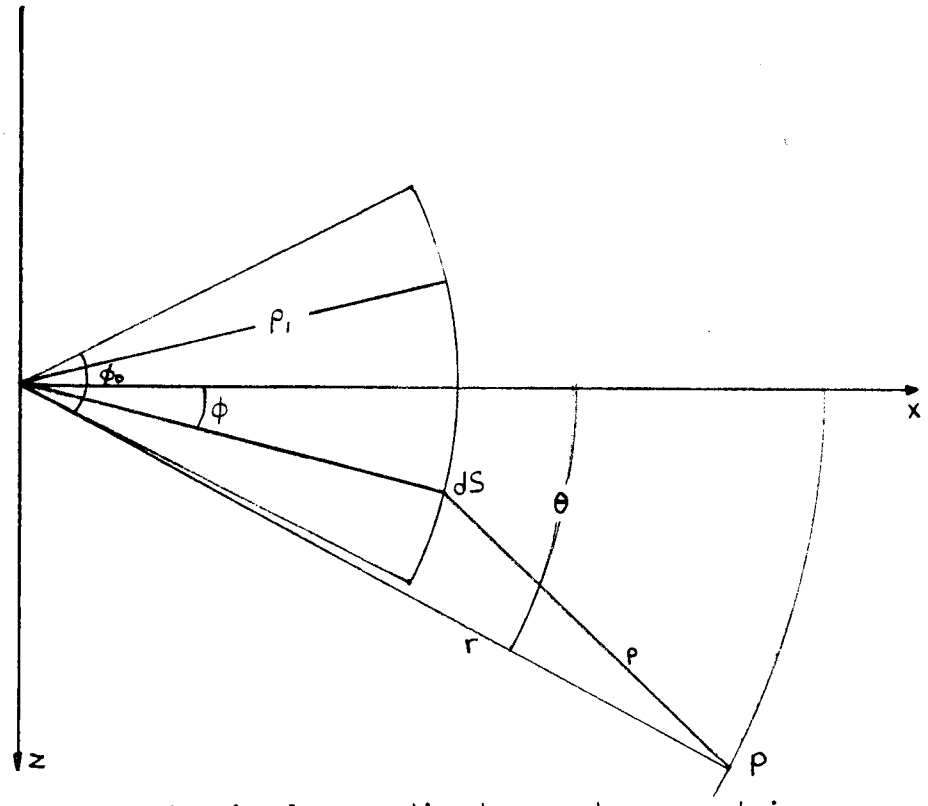

Figure 2.3. Spherical coordinate system used in calculating radiation patterns.

or

$$E_y = (2\pi)^2 \Pi_y . \tag{2.38}$$

At point P, which is large compared to the wavelength and dimensions of the horn, Hertzian vector IIy' can be calculated by Huygens principle. This is written in the form

$$\Pi_y' = \frac{1}{4\pi}\iint \frac{1}{\rho}\left[\frac{j\omega}{c}\Pi_y \cos(n',\rho) + \frac{2\Pi_y}{2\rho}\right] e^{-j(\omega/c)\rho}\, dS , \tag{2.39}$$

where n' is the inner normal to the surface element dS.

The integration is taken over the mouth but not the outer metallic surface of the horn. The field distribution is not known here.

We substitute the value for IIy into (2.39) to obtain

$$\Pi_4' = \frac{B}{4\pi}\left(\frac{c}{\omega}\right)^2 \int_0^a \int_{-\phi_0/2}^{\phi_0/2} \frac{j\omega}{\rho c}$$

$$\cdot\left[K_{\pi/\phi_0}\left(\frac{\omega\rho_1}{c}\right)\cos(\phi-\theta) + K_{\pi/\phi_0}\left(\frac{\omega\rho_1}{c}\right)\right]\cos(\pi\phi/\phi_0)e^{-(j\omega/c)\rho}\rho_1 d\phi dy. \quad (2.40)$$

K_{π/ϕ_0} and K'_{π/ϕ_0} can be approximated by their asymptotic forms and ρ can be approximated for large values of r, by

$$\rho = \sqrt{r^2 + \rho_1^2 - 2r\rho_1\cos(\phi-\theta)} = r - \rho_1\cos(\phi-\theta). \quad (2.41)$$

Using these, we can write E_θ as

$$E_\theta = \frac{a\sqrt{\rho_1}}{r}(1+\cos\theta)\, e^{-(2\pi j)(r+\rho_1)}$$

$$\cdot\int_{-\phi_0/2}^{\phi_0/2} \cos(\pi\phi/\phi_0)\, e^{j(2\pi\rho_1)\cos(\phi-\theta)}\, d\phi. \quad (2.42)$$

Taking the absolute value of E_θ , we write $|E_\theta|$ as

$$|E_\theta| = \frac{a\sqrt{\rho_1}}{r}(1+\cos\theta)$$

$$\left|\int_{-\phi_0/2}^{\phi_0/2} \cos(\pi\phi/\phi_0)\, e^{j2\pi\rho_1\cos(\phi-\theta)}\, d\phi\ .\right| \quad (2.43)$$

The calculation of $|E_\theta|$ is given by PROGRAM FIVE.

CHAPTER III

RESULTS AND DISCUSSION

All of the following figures and tables may be found in the Appendix.

We now consider a horn with the flare angle ϕ_o, equal to 90 degrees, the width equal to λ, and the length equal to 6λ. The range for θ will befrom 0 to 90 degrees and since our plot is symmetrical, the effective range will 180 degrees. The results for this horn are contained in Table B.1 and plotted in figure A.1.

The exact solution shows a broad pattern with lobes absent, directed along the axis of the horn. This solution differs from the measured pattern because:

A). The sides of the horn are assumed to extend to infinity.

B). The edge effects are neglected.

C). All radiation is assumed to come from the mouth of the horn.

PROGRAM FIVE is used to calculate the exact solution.

The one section Fresnel solution for the same horn differs greatly from the exact solution. This results primarily from the large phase error associated with a horn of such wide flare. When the horn becomes broken into two sections, the phase error is reduced considerably

and the two section Fresnel solution more closely approaches the exact solution. However, four lobes now appear on each side. The three section Fresnel solution comes even closer to the exact solution and also has four lobes on each side.

Next, we look at the horn with the flare angle of 60 degrees, the width equal to λ , and the length equal to 6λ. θ will range from 0 to 90 degrees. The results for this are contained in Table B.2 and plotted in Figure A.2.

The Fresnel solution for one, two, and three sections comes even closer to the exact solution, however, the exact solution still has no lobes. This pattern was found to repeat itself for flare angles equal to 45, 30, and 20 degrees. The results for these are in Tables B.3, B.4, and B.5 and the plots are given in figures A.3, A.4, and A.5. Plots of the measured solutions are given in Figures A.6 through A.11 [3]. PROGRAM ONE was used to calculate the Fresnel approximation solution and PROGRAM FIVE was used to calculate the exact solution.

PROGRAM FIVE was also used to calculate the maximum on axis field, on θ equal to zero, as a function of the flare angle ϕ_o . At this maximum, the horn radiates most efficiently, the shape of the pattern is narrow, and there is almost no back radiation. This flare angle was calculated by the exact method to be between 40 and 60

degrees and was measured to be the same. The calculated values are given in Table B.6 and the plots in Figures A.12 and A.13 [3].

Several patterns result from the derivations and data. As the angle of flare decreases, the Fresnel method gives a good approximation for the E-field. This approximation becomes better when the horn is divided into sections. For flare angles less than 60 degrees, the exact method gives a pattern identical to the measured one. The horn was found to radiate most efficiently at an angle between 40 and 60 degrees. This also corresponds with the measured value.

In conclusion, the exact method works well for flare angles less than 60 degrees, and the Fresnel method works better for angles greater than 60 degrees. The exact method, which used the asymptotic form of the Hankel function, takes much less computer time than does the Fresnel method.

BIBLIOGRAPHY

1. Constantine A. Balanis, "Antenna Theory, Design and Analysis," Harper and Row, Publishers, New York, N.Y. (1982).

2. W.L. Barrow and L.J. Chu, "Theory of the Electromagnetic Horn," Proceedings of the I.R.E., January, (1939) pp 51-64.

3. W.L. Barrow and F.D. Lewis, "The Sectoral Electromagnetic Horn," Proceedings of the I.R.E., January, (1939) pp 41-50.

APPENDICES

APPENDIX A

FIGURES

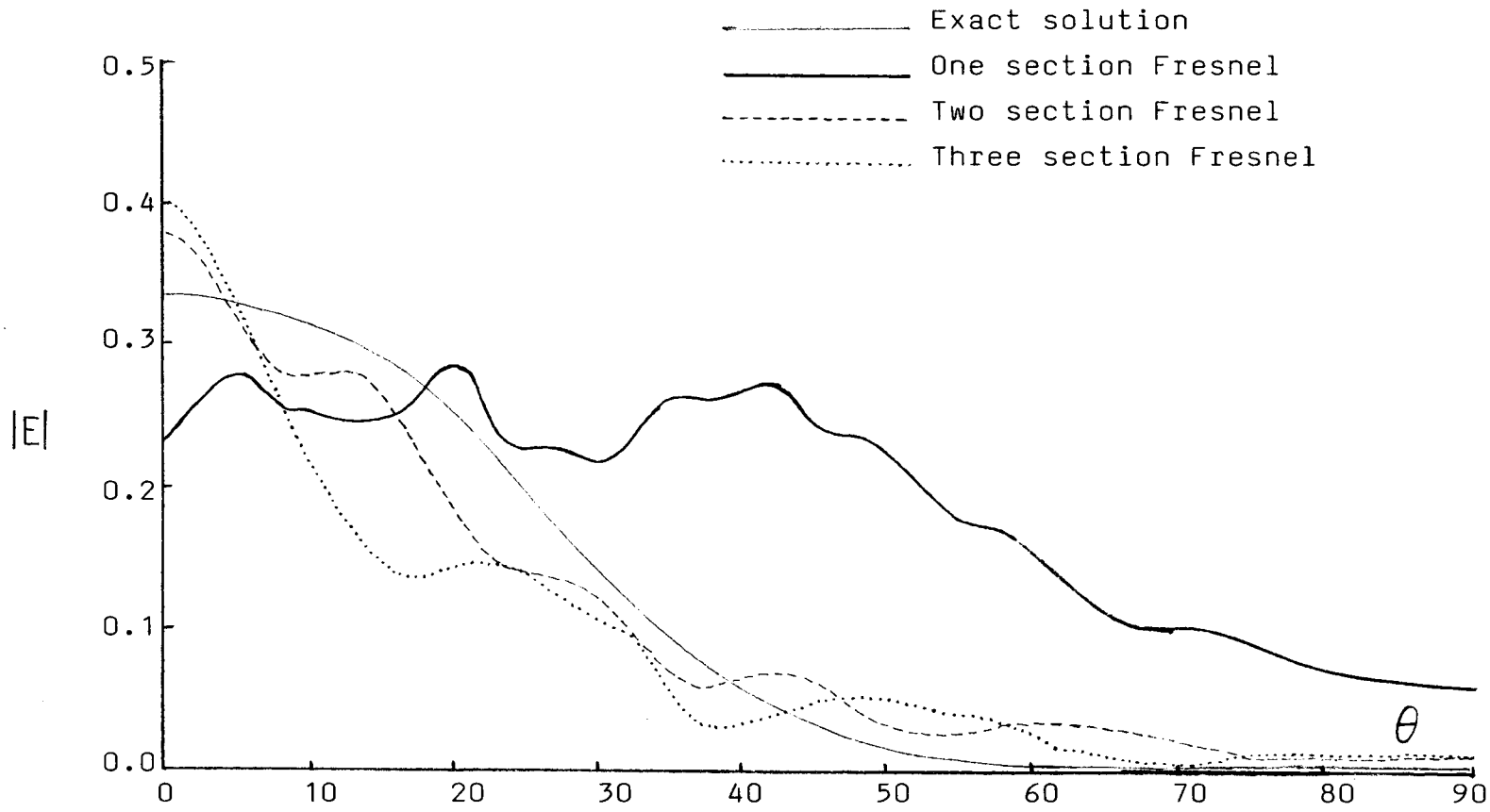

Figure A.1. The one, two, and three section Fresnel approximation and the exact solution for a horn of 90° flare angle, length of 6λ, and width of 1λ.

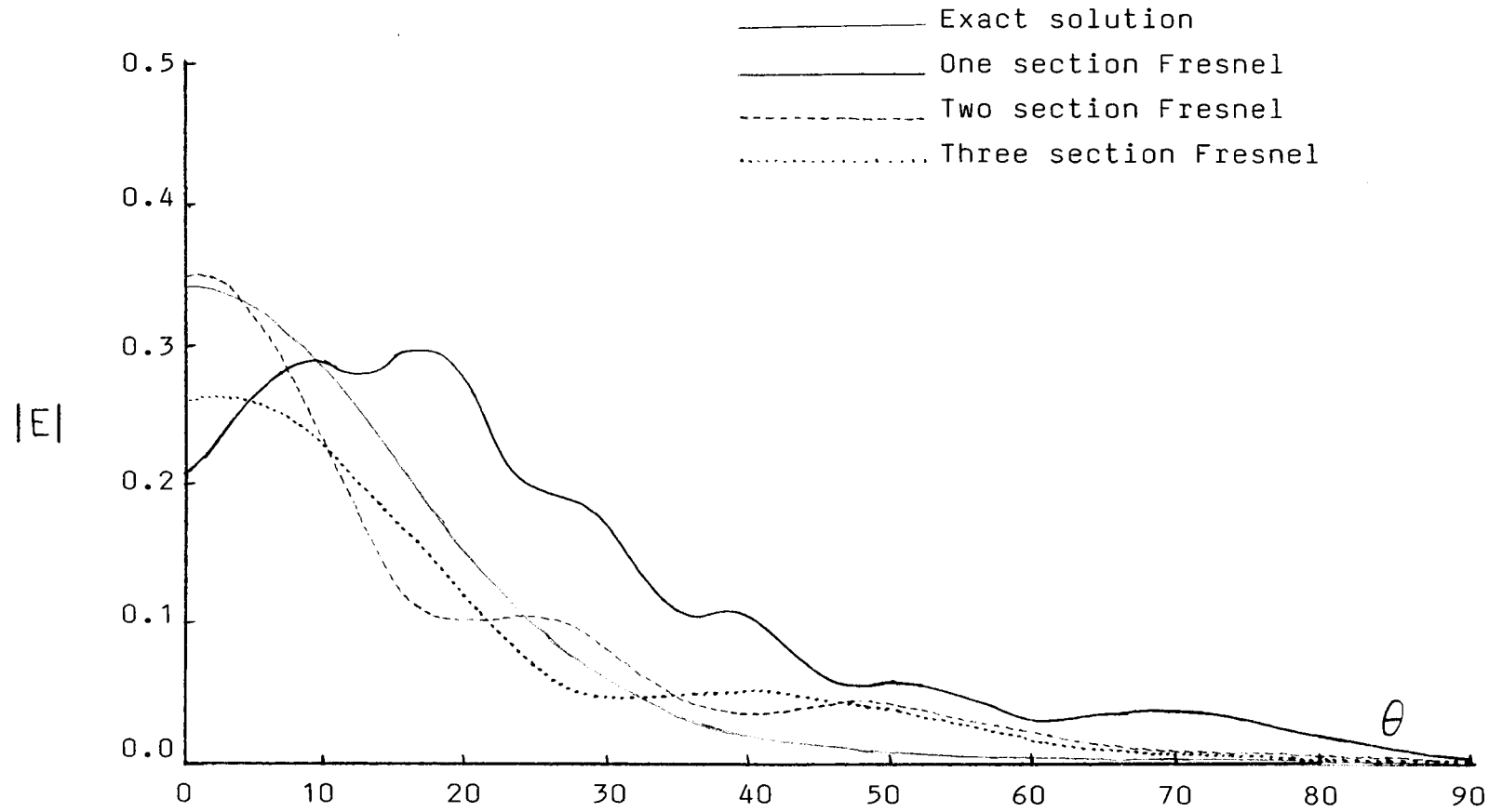

Figure A.2. The one, two, and three section Fresnel approximation and the exact solution for a horn of 60° flare angle, length of 6λ, and width of 1λ.

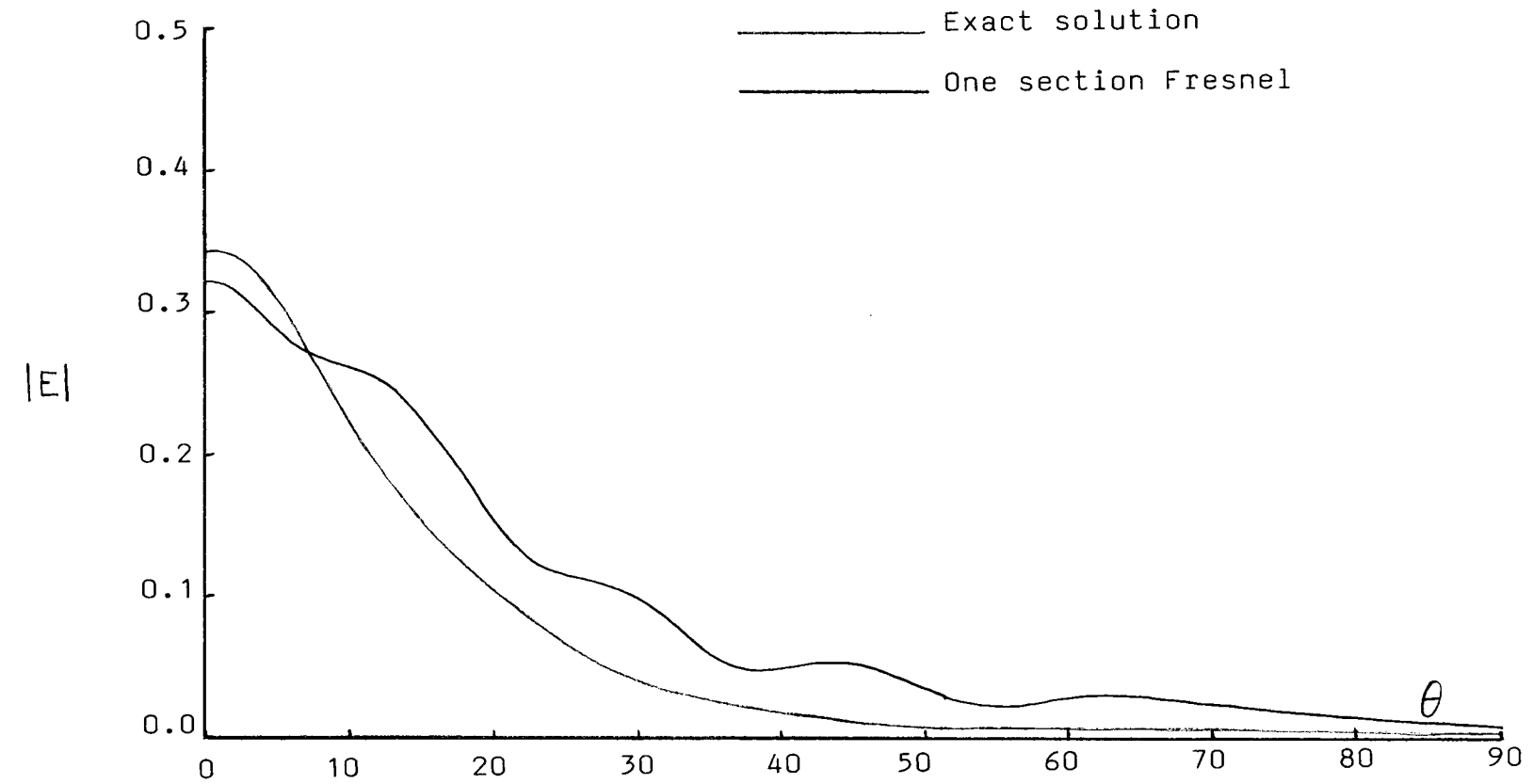

Figure A.3. The one section Fresnel approximation and the exact solution for a horn of 45° flare angle, length of 6λ, and width of 1λ.

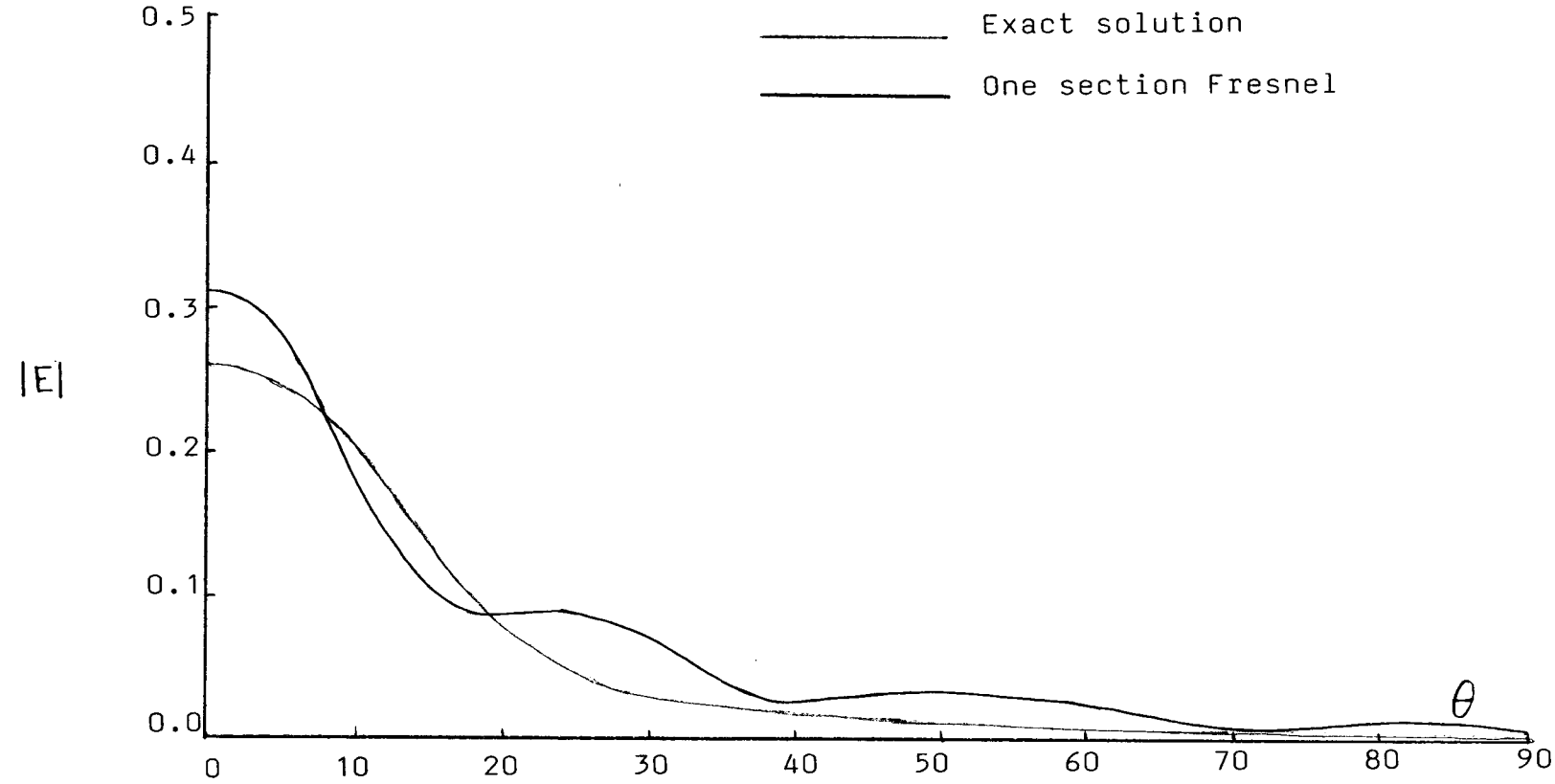

Figure A.4. The one section Fresnel approximation and the exact solution for a horn of 30° flare angle, length of 6λ, and a width of 1λ.

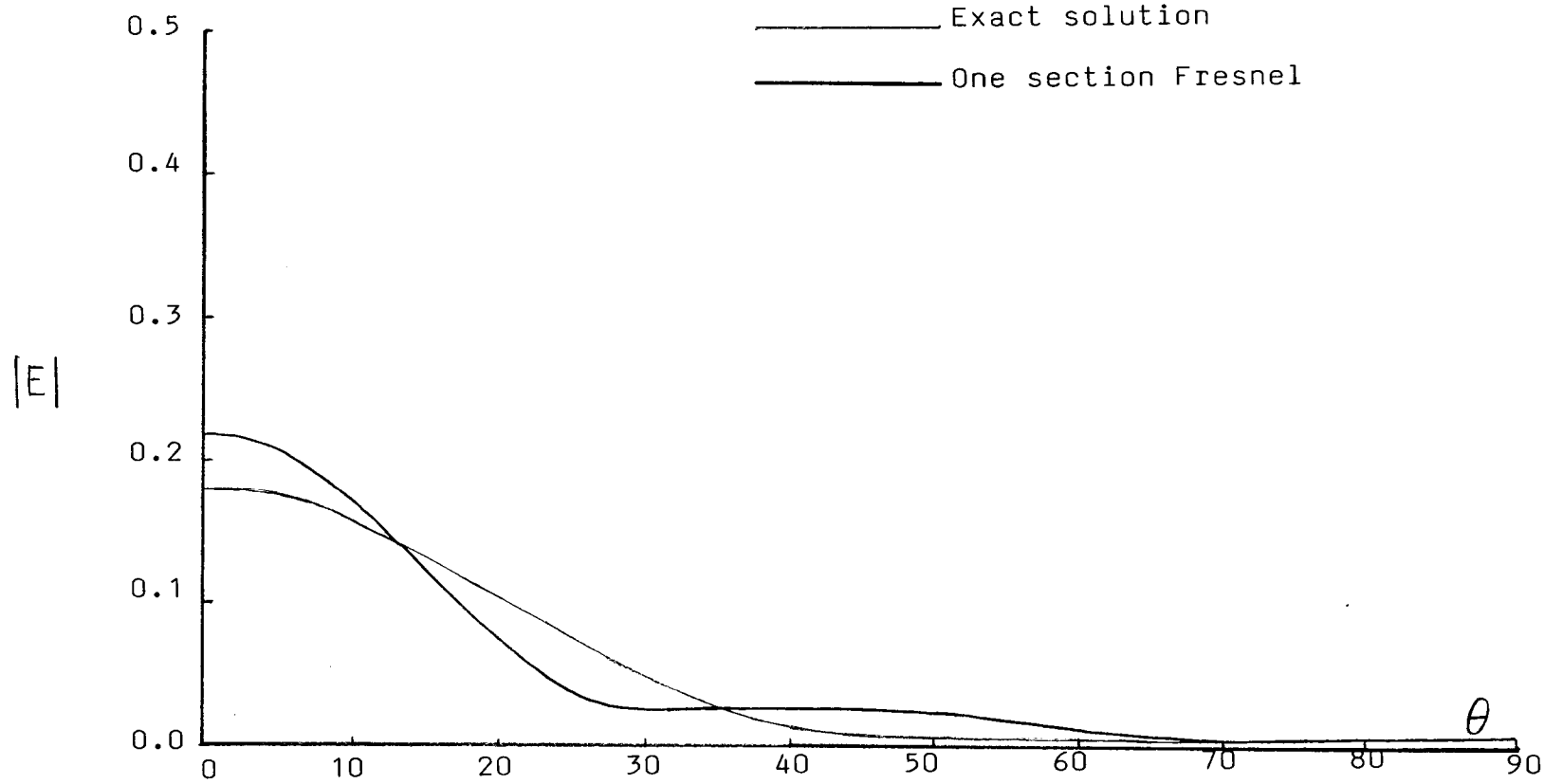

Figure A.5. The one section Fresnel approximation and the exact solution for a horn of 20° flare angle, length of 6λ, and a width of 1λ.

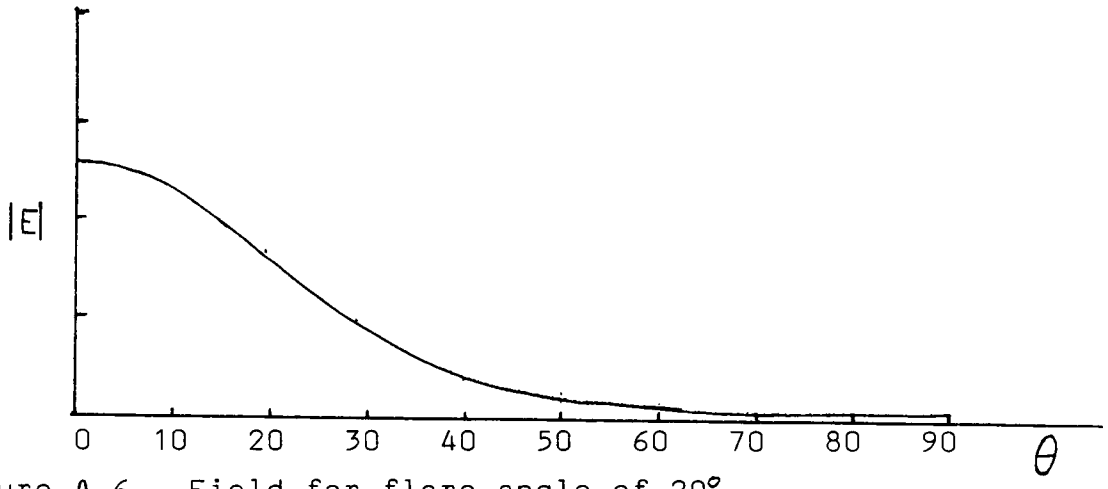

Figure A.6. Field for flare angle of 20°.

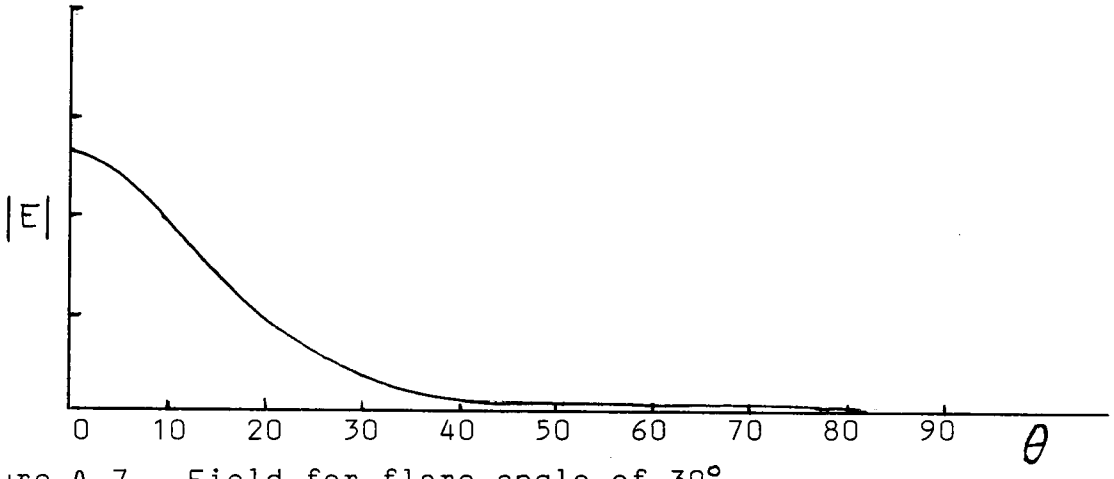

Figure A.7. Field for flare angle of 30°.

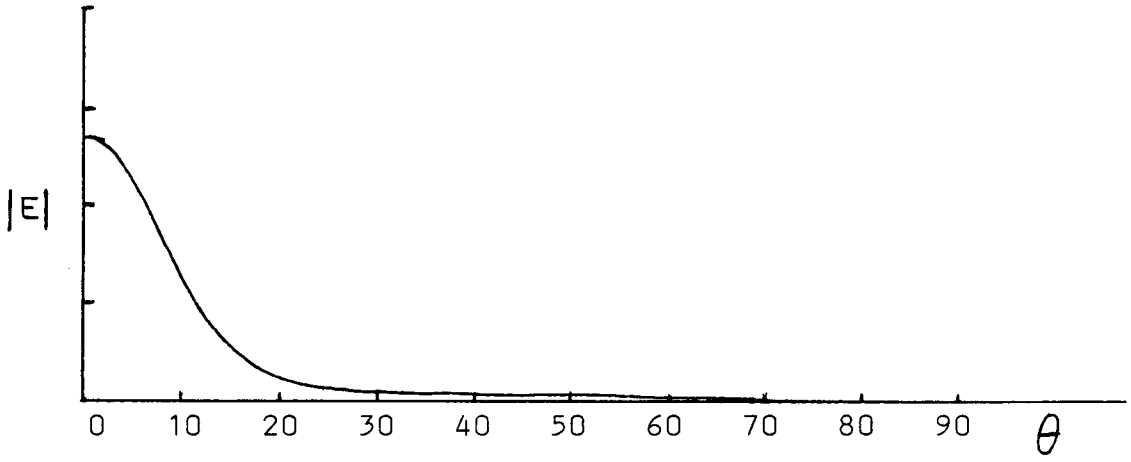

Figure A.8. Field for a flare angle of 40°.

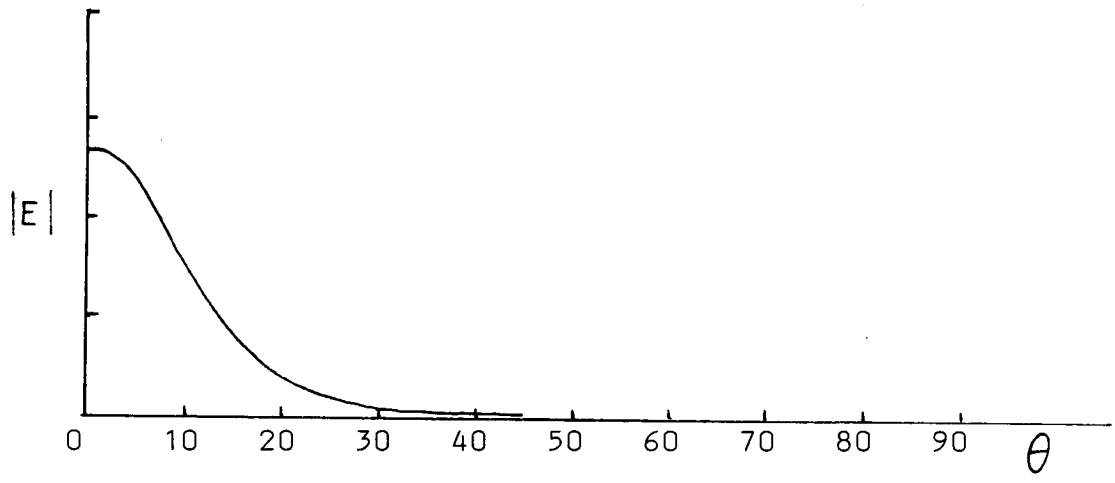

Figure A.9. Field for a flare angle of 50°.

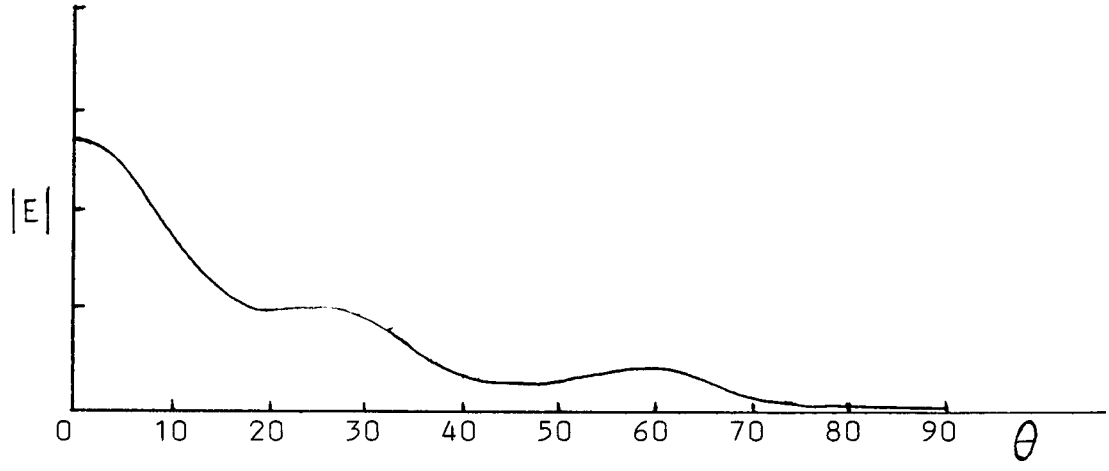

Figure A.10. Field for a flare angle of 70°.

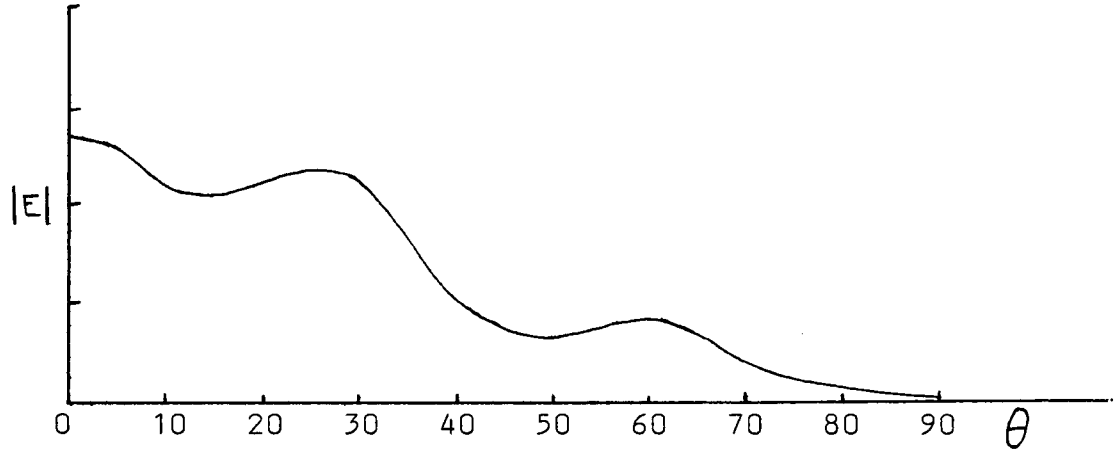

Figure A.11 Field for a flare angle of 90°.

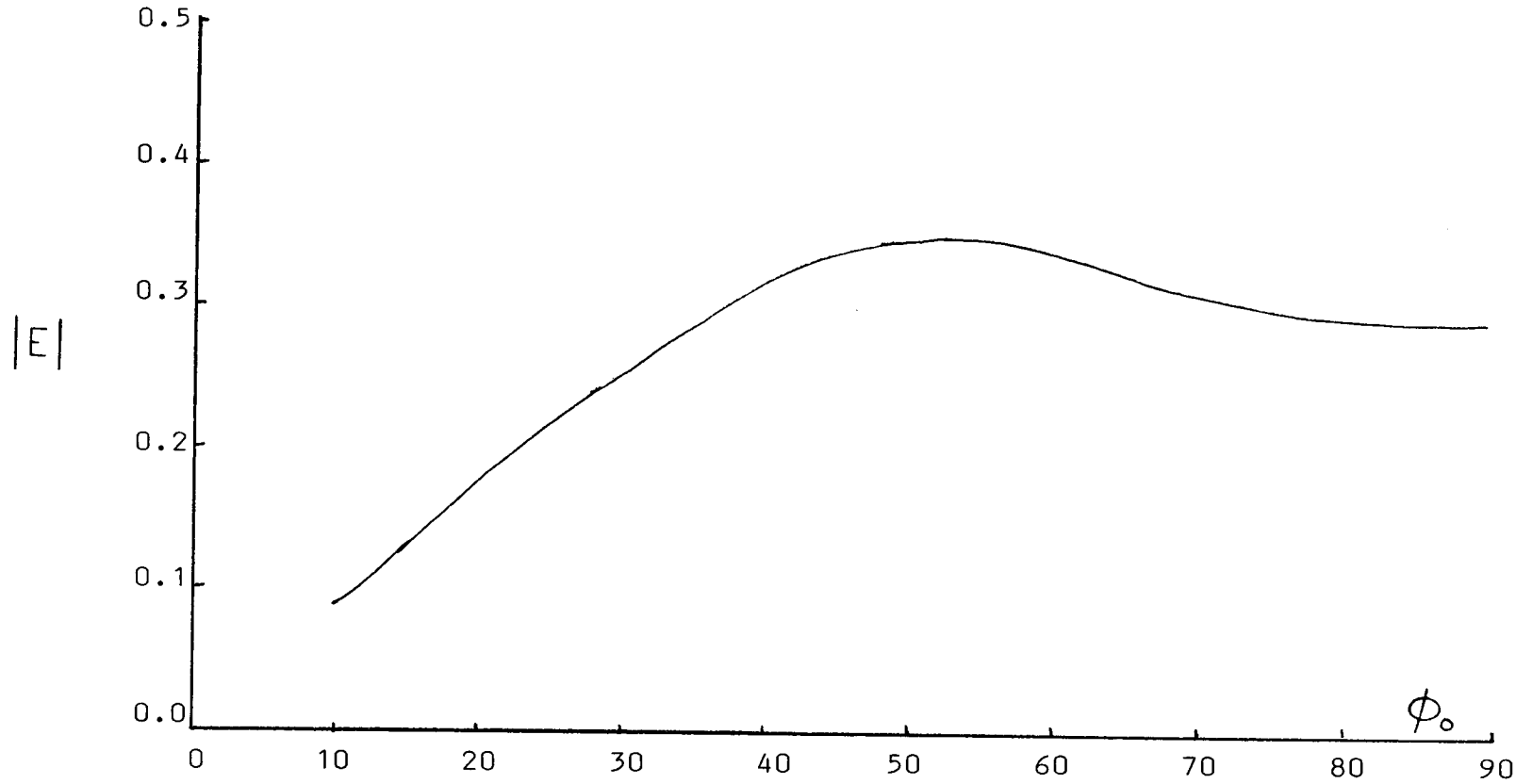

Figure A.12. Calculated on axis field as a function of flare angle.

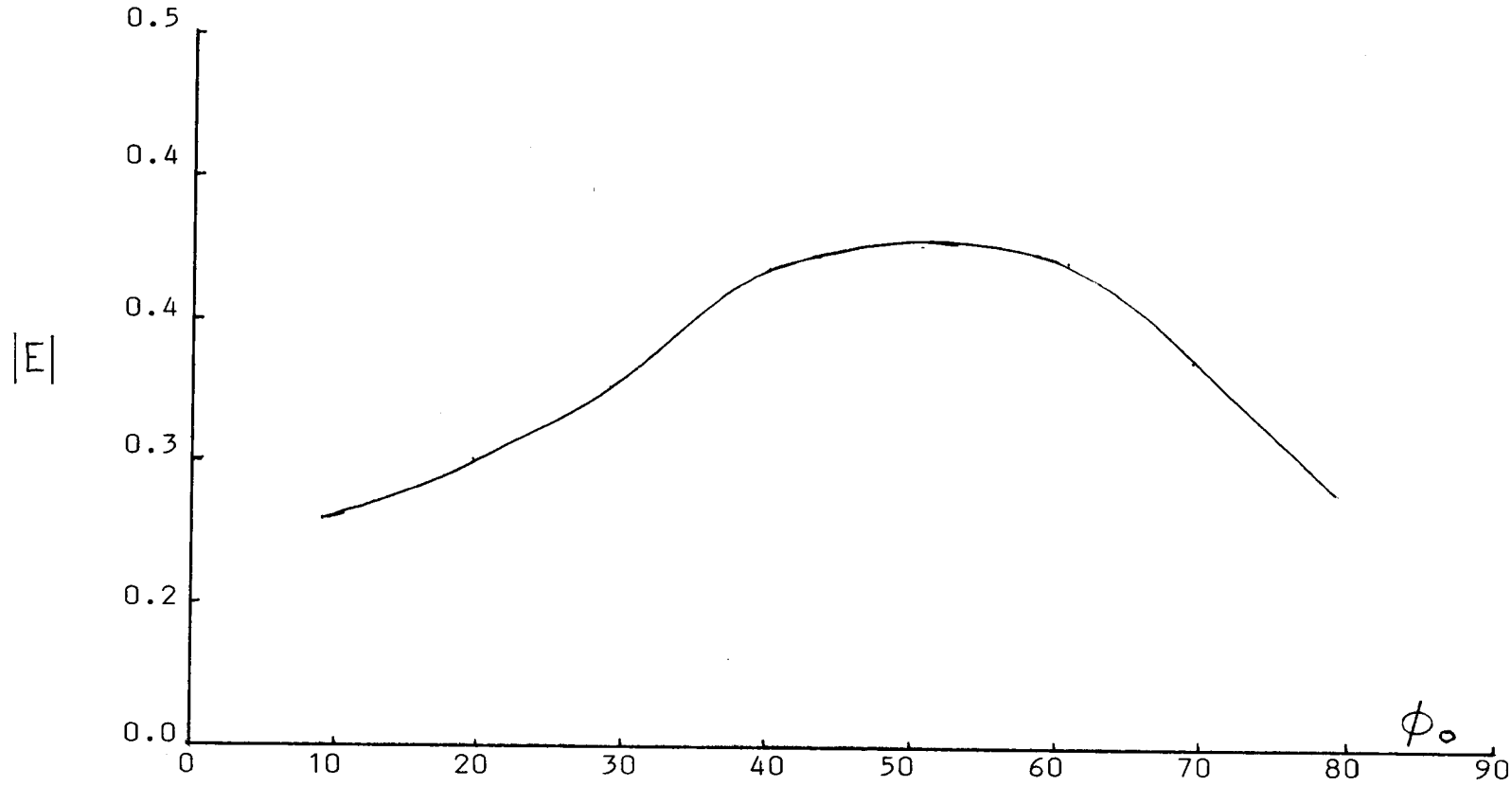

Figure A.13. Maximum on axis field as a function of flare angle

APPENDIX B

TABLES

Table B.1. One, two, and three section Fresnel approximations and exact solution for a horn of 90° flare angle, length of 6λ, and width of 1λ.

Theta	1 section	2 section	3 section	Exact
0	.23658	.38115	.40685	.33681
2	.25307	.36632	.38170	.33471
4	.27917	.33478	.34405	.32940
6	.27529	.30152	.30122	.32290
8	.25525	.28154	.25751	.31639
10	.25033	.27922	.21950	.30949
12	.24988	.28321	.18717	.30116
14	.24622	.27768	.16096	.29102
16	.25095	.25563	.14444	.27967
18	.27720	.22014	.13967	.26740
20	.28551	.18190	.14220	.25295
22	.25385	.15489	.14480	.23454
24	.22664	.14565	.14295	.21225
26	.22676	.14481	.13522	.18856
28	.22560	.13967	.12204	.16611
30	.21780	.12542	.10481	.14534
32	.23090	.10342	.07376	.12511
34	.26031	.07966	.05508	.10522
36	.26767	.06302	.03958	.08714
38	.25978	.06002	.03145	.07244
40	.26713	.06508	.03283	.06085
42	.27279	.06904	.03916	.05082
44	.25521	.06797	.04562	.04138
46	.23609	.06166	.05029	.03294
48	.23288	.04367	.05263	.02644
50	.22581	.03290	.05272	.02209
52	.20380	.03446	.05088	.01900
54	.18259	.02201	.04757	.01610
56	.17478	.02505	.04322	.01304
58	.17032	.02942	.03827	.01011
60	.15834	.03267	.03311	.00783
62	.13974	.03406	.01641	.00652
64	.12513	.03367	.01246	.00599
66	.11893	.03185	.00945	.00571
68	.11658	.02907	.00782	.00534
70	.11288	.02577	.00767	.00478
72	.10606	.02233	.00849	.00407
74	.09724	.01906	.00963	.00330
76	.08840	.01617	.01070	.00255
78	.08099	.01378	.01157	.00189

Table B.1. (Continued)

Theta	1 section	2 section	3 section	Exact
80	.07547	.01194	.01220	.00133
82	.07156	.01062	.01258	.00089
84	.06867	.00917	.01275	.00056
86	.06628	.00910	.01271	.00030
88	.06404	.00866	.01251	.00019
90	.06193	.00833	.01215	.00014

Table B.2. One, two, and three section Fresnel approximations and exact solution for a horn of 60° flare angle, length of 6λ, and width of 1λ.

Theta	1 section	2 section	3 section	Exact
0	.21940	.35020	.26398	.34116
2	.22882	.34755	.26377	.33819
4	.25333	.33093	.26021	.32900
6	.27970	.30216	.25230	.31760
8	.29175	.26433	.24019	.30208
10	.28623	.22149	.22456	.28301
12	.27908	.17852	.20613	.25960
14	.28663	.14108	.18550	.23193
16	.29943	.11511	.16324	.20176
18	.29468	.10345	.14020	.17214
20	.26484	.10194	.11721	.14599
22	.22559	.10337	.09527	.12449
24	.20199	.10320	.06848	.10666
26	.19746	.09967	.06016	.09059
28	.19070	.09226	.05145	.07514
30	.16804	.08133	.04973	.06066
32	.13589	.06803	.04470	.04843
34	.11299	.05419	.04714	.03951
36	.10911	.04233	.04896	.03364
38	.11070	.03621	.04993	.02935
40	.10343	.03791	.05021	.02522
42	.08603	.04338	.04992	.02075
44	.06695	.04852	.04897	.01627
46	.05783	.05174	.04724	.01255
48	.06036	.04106	.04477	.01025
50	.06430	.04052	.04170	.00932
52	.06278	.03830	.03816	.00901
54	.05521	.03482	.03436	.00857
56	.04442	.03051	.03043	.00774
58	.03490	.02576	.02653	.00655
60	.03095	.02096	.02274	.00518
62	.03266	.01641	.01579	.00385
64	.03608	.01246	.01252	.00278
66	.03833	.00945	.00966	.00220
68	.03852	.00782	.00730	.00214
70	.03685	.00767	.00558	.00237
72	.03390	.00849	.00467	.00262
74	.03031	.00963	.00456	.00279
76	.02664	.01070	.00498	.00286
78	.02330	.01157	.00557	.00286

Table B.2. (Continued)

Theta	1 section	2 section	3 section	Exact
80	.02053	.01220	.00615	.00280
82	.01837	.01258	.00663	.00270
84	.01680	.01275	.00696	.00259
86	.01567	.01271	.00716	.00248
88	.01486	.01251	.00721	.00238
90	.01427	.01215	.00714	.00297

Table B.3 One section Fresnel approximation and exact solution for a horn of 45° flare angle, length of 6λ, and width of 1λ.

Theta	1 section	Exact
0	.32184	.34400
2	.31299	.33776
4	.29120	.31991
6	.26862	.29287
8	.25706	.26019
10	.25721	.22591
12	.25816	.19369
14	.24826	.16591
16	.22296	.14317
18	.18608	.12436
20	.14823	.10768
22	.12304	.09173
24	.11658	.07601
26	.11904	.06132
28	.11743	.04842
30	.10636	.03847
32	.08725	.03191
34	.06588	.02808
36	.05108	.02553
38	.04940	.02303
40	.05537	.02000
42	.05994	.01653
44	.05931	.01295
46	.05333	.00975
48	.04367	.00747
50	.03290	.00646
52	.02446	.00644
54	.02201	.00676
56	.02505	.00693
58	.02942	.00680
60	.03267	.00638
62	.03406	.00573
64	.03367	.00494
66	.03185	.00410
68	.02907	.00326
70	.02577	.00249
72	.02233	.00180
74	.01906	.00124
76	.01617	.00083
78	.01378	.00061

Table B.3. (Continued)

Theta	1 section	Exact
80	.01194	.00060
82	.01062	.00070
84	.00971	.00079
86	.00910	.00086
88	.00866	.00088
90	.00833	.00087

Table B.4. One section Fresnel approximation and exact solution for a horn of 30° flare angle, length of 6λ, and width of 1λ.

Theta	1 section	Exact
0	.31419	.26274
2	.30796	.25991
4	.28987	.25158
6	.26164	.23831
8	.22603	.22056
10	.18667	.19957
12	.14801	.17635
14	.11532	.15206
16	.09415	.12785
18	.08704	.10483
20	.08948	.08398
22	.09392	.06612
24	.09538	.05192
26	.09200	.04174
28	.08377	.03568
30	.07170	.03185
32	.05733	.02983
34	.04262	.02817
36	.03013	.02623
38	.02363	.02379
40	.02516	.02092
42	.03067	.01775
44	.03061	.01449
46	.03959	.01135
48	.04106	.00858
50	.04052	.00618
52	.03830	.00460
54	.03482	.00399
56	.03051	.00421
58	.02576	.00475
60	.02096	.00528
62	.01641	.00568
64	.01246	.00591
66	.00945	.00598
68	.00782	.00593
70	.00767	.00579
72	.00849	.00557
74	.00963	.00532
76	.01070	.00505
78	.01157	.00478

Table B.4. (Continued)

Theta	1 section	Exact
80	.01220	.00451
82	.01258	.00426
84	.01275	.00404
86	.01271	.00385
88	.01251	.00368
90	.01215	.00355

Table B.5. One section Fresnel approximation and exact solution for a horn of 20° flare angle, length of 6λ , and width of 1λ .

Theta	1 section	Exact
0	.22120	.18017
2	.21907	.17923
4	.21307	.17645
6	.20334	.17198
8	.19026	.16568
10	.17435	.15801
12	.15621	.14906
14	.13653	.13908
16	.11602	.12832
18	.09543	.11702
20	.07551	.10544
22	.05711	.09382
24	.04128	.08238
26	.02973	.07133
28	.02492	.06082
30	.02699	.05101
32	.03218	.04199
34	.03748	.03385
36	.04166	.02665
38	.04435	.02044
40	.04554	.01128
42	.04536	.01126
44	.04399	.00855
46	.04167	.00729
48	.03862	.00726
50	.03507	.00786
52	.03120	.00860
54	.02720	.00924
56	.02322	.00968
58	.01939	.00993
60	.01579	.01000
62	.01252	.00992
64	.00966	.00972
66	.00730	.00943
68	.00558	.00908
70	.00467	.00869
72	.00456	.00829
74	.00498	.00788
76	.00557	.00748
78	.00615	.00710

Table B.5. (Continued)

Theta	1 section	Exact
80	.00663	.00675
82	.00696	.00642
84	.00716	.00612
86	.00721	.00586
88	.00714	.00563
90	.00695	.00542

Table B.6. Maximum on axis field at θ equal to 0, length of 6λ , and width of 1λ.

Flare Angle	Field
10	.09068
12	.10877
14	.12680
16	.14474
18	.16255
20	.18017
22	.19755
24	.21459
26	.23121
28	.24730
30	.26274
32	.27740
34	.29114
36	.30382
38	.31529
40	.32541
42	.33405
44	.34110
46	.34648
48	.35041
50	.35210
52	.35241
54	.35123
56	.34785
58	.34528
60	.34116
62	.33683
64	.33272
66	.32925
68	.32679
70	.32556
72	.32562
74	.32686
76	.32900
78	.33164
80	.33431

APPENDIX C

BASIC PROGRAMS

```
REM     THIS IS PROGRAM ONE.  IT FINDS THE APPROXIMATE
REM     SOLUTION FOR THE FIELDS OF AN E-PLANE HORN BY
REM     THE USE OF SINE AND COSINE FRESNEL INTEGRALS.  THE
REM     INTEGRALS ARE EVALUATED BY SIMPSON'S METHOD IN
REM     SUBROUTINES 5000 AND 6000.
REM
REM
REM
10      CLEAR
20      INPUT"FLARE ANGLE";FLANG
30      INPUT"R01";R01
40      INPUT"ARE";ARE
50      INPUT"WIDTH OF HORN";WID
REM
60      FOR THETA=0 TO 90  STEP 2
REM
70      PI=3.1415927
80      TRAD=THETA*PI/180
90      FRAD=FLANG*PI/180
REM
1000    B1=2*R01*TAN(FRAD/2)
1010    W=(-B1/2-R01*SIN(TRAD))*SQR(2/R01)
REM
1020    GOSUB 5000
1030    GOSUB 6000
```

```
1040    AAA=CFRES
1050    BBB=SFRES
REM
1060    W=(B1/2-RO1*SIN(TRAD))*SQR(2/RO1)
REM
1070    GOSUB 5000
1080    GOSUB 6000
1090    CCC=CFRES
1100    DDD=SFRES
REM
1110    MAX=SQR((CCC-AAA)**2+(DDD-BBB)**2)
REM
1120    EMAX=((WID/2*ARE*PI)*SQR(2*RO1))*(1+COS(TRAD))*MAX
REM
1130    ONE(THETA)=EMAX
REM
REM
REM     HORN WITH FLARE ANGLE EQUAL TO FLANG/2
REM
REM
2000    RO2=RO1*COS(FRAD/4)
2010    B2=2*RO1*SIN(FRAD/4)
2020    W=(-B2/2-RO2*SIN(TRAD))*SQR(2/RO2)
REM
2030    GOSUB 5000
```

```
2040    GOSUB 6000
2050    AAA=CFRES
2060    BBB=SFRES
REM
2070    W=(B2/2-RO2*SIN(TRAD)O*SQR(2/RO2)
REM
2080    GOSUB 5000
2090    GOSUB 6000
2100    CCC=CFRES
2110    DDD=SFRES
REM
2120    MAX=SQR((CCC-AAA)**2+(DDD-BBB)**2)
REM
2130    EMAX=((WID/2*ARE*PI)*SQR(W*RO2))*(1+COS(TRAD))*MAX
REM
2140    TWO(THETA)=EMAX
REM
REM
REM     HORN WITH FLARE ANGLE EQUAL TO FLANG/3
REM
REM
3000    RO3=RO1*COS(FRAD/6)
3010    B3=2*RO1*SIN(FRAD/6)
3020    W=(-B3/2-RO3*SIN(TRAD))*SQR(2/RO3)
```

```
REM
3030    GOSUB 5000
3040    GOSUB 6000
3050    AAA=CFRES
3060    BBB=SFRES
REM
3070    W=(B3/2-RO3*SIN(TRAD))*SQR(2/RO3)
REM
3080    GOSUB 5000
3090    GOSUB 6000
3100    CCC-CFRES
3110    DDD=SFRES
REM
3120    MAX=SQR((CCC-AAA)**2+(DDD-BBB)**2)
REM
3130    EMAX=((WID/2*ARE*PI)*SQR(2*RO3))*(1+COS(TRAD))*MAX
REM
3140    FRE(THETA)=EMAX
REM
3150    NEXT THETA
REM
REM
REM
4000    G=0
4010    PRINT"ONE(";G")=";ONE(G)
```

```
4020    PRINT"TWO(";G")=";TWO(G)
4030    PRINT"FRE(";G")=";FRE(G)
4040    G=G+2
4050    IF G=90 THEN 4080
4060    INPUT"1 TO CONTINUE";SWITCH
4070    IF SWITCH=1 THEN 4010
4080    END
REM
REM
REM
5000    A=0
5010    B=W
5020    PI=3.1415927
5030    N=100
5040    D=(B-1)/N
5050    FOR I=0 TO N
5060    X=A+I*D
5070    F=COS((PI*X*X)/2)
5080    T=L/2-INT(L/2)
5090    IF T.GT.0 AND T.LT.N THEN LET P=4*F
5100    IF T.EQ.0 AND L.LT.(N-1) THEN LET P=2*F
5110    IF L.EQ.0 OR L.EQ.N THEN LET P=F
5120    L=L+1
5130    R=R+P
5140    NEXT I
```

```
5150    CFRES=D*R/3
5160    RETURN
REM
REM
REM
6000    A=0
6010    B=W
6020    PI=3.1415927
6030    N=100
6040    D=(B-A)/N
6050    FOR I=0 TO N
6060    X=A+I*D
6070    F=SIN((PI*X*X)/2)
6080    T=L/2-INT(L/2)
6090    IF T.GT.0 AND T.LT.N THEN LET P=4*F
6100    IF T.EQ.0 AND T.LT.(N-1) THEN LET P=2*F
6110    IF L.EQ.0 OR L.EQ.N THEN LET P=F
6120    L=L+1
6130    R=R+P
6140    NEXT I
6150    SFRES=D*R/3
6160    RETURN
```

```
REM     PROGRAM TWO APPROXIMATE SOLUTION TO EPHI
10      CLEAR
20      INPUT"WIDTH OF HORN";WID
30      INPUT"RO1";RO1
40      INPUT"ARE";ARE
50      INPUT"FLARE ANGLE";FLANG
60      FOR THETA=0 TO 90  STEP 2
70      PI=3.1415927
80      FRAD=FLANG*PI/180
90      TRAD=THETA*PI/180
REM
100     B1=2*RO1*TAN(FRAD/2)
110     W=(-B1/2)*SQR(2/RO1)
120     GOSUB 5000
130     GOSUB 6000
140     AAA=CFRES
150     BBB=SFRES
REM
160     W=(B1/2)*SQR(2/RO1)
170     GOSUB 5000
180     GOSUB 6000
190     CCC=CFRES
200     DDD=SFRES
```

```
REM
210     MAX=SQR((CCC-AAA)**2+(DDD-BBB)**2)
REM
220     CNT=(WID/8*ARE)*SQR(2*PI*PI*RO1)
REM
230     MID=(COS((WID*PI)*SIN(TRAD)))/(((WID*PI)*SIN(TRAD))
        **2-(PI/2)**2
REM
240     EMAX=MAX*CNT*MID*(1+COS(TRAD))
REM
250     PRINT"EMAX(";THETA")=";EMAX
REM
260     NEXT THETA
REM
270     END
REM
REM
REM
5000    A=0
5010    B=2
5020    PI=3.1415927
5030    N=100
5040    D=(B-A)/N
5050    FOR I=0 TO N
5060    X=A+1*D
5070    F=COS((PI*X*X)/2)
```

```
5080    T=L/2-INT(L/2)
5090    IF T.GT.0 AND T.LT.N THEN LET P=4*F
5110    IF T.EQ.0 AND L.LT.(N-1) THEN LET P=2*F
5110    IF L.EQ.0 OR L.EQ.N THEN LET P=F
5120    L=L+1
5130    R=R+P
5140    NEXT I
5150    CFRES=D*R/3
5160    RETURN
REM
REM
REM
6000    A=0
6010    B=W
6020    PI=3.1415927
6030    N=100
6040    D=(B-A)/N
6050    FOR I=0 TO N
6060    X=A+I*D
6070    F=SIN((PI*X*X)/2)
6080    T=L/2-INT(L/2)
6090    IF T.GT.0 AND T.LT.N THEN LET P=4*F
6100    IF T.EQ.0 AND L.LT.(N-1) THEN LET P=2*F
6110    IF L.EQ.0 OR L.EQ.N THEN LET P=F
6120    L=L+1
```

```
6130      R=R+P
6140      NEXT I
6150      SFRES=D*R/3
6160      RETURN
```

```
REM   THIS IS PROGRAM THREE.  IT USES THE ASYMPTOTIC
REM   FORM OF THE HANKEL FUNCTION TO CALCULATE THE MAXIMUM
REM   VALUE OF ETHETA INSIDE OF AN E-PLANE SECTORAL HORN
REM   FOR LARGE VALUE OF RO1.
REM
REM   VARIABLE LIST:
REM   ETHETA    THE MAXIMUM VALUE OF ETHETA.
REM   RO1       THE DISTANCE FROM THE APEX TO THE APERTURE.
REM   FLANG     THE FLARE ANGLE IN DEGREES.
REM   PHI       THE ANGLE BETWEEN THE MAIN AXIS AND THE
REM             OBSERVATION POINT.
REM
10    CLEAR
20    INPUT"RO1";RO1
30    INPUT"FLARE ANGLE";FLANG
40    INPUT"PHI";PHI
REM
50    PI=3.1415927
60    ETHETA=(2*PI*COS(PI*PHI/FLANG))*SQR(1/PI*PI*RO1)
70    PRINT"ETHETA="ETHETA
80    END
```

```
REM   THIS IS PROGRAM FOUR.  IT USES THE ASYMPTOTIC FORM
REM   OF THE HANKEL FUNCTION TO CALCULATE THE ABSOLUTE
REM   VALUE OF EPHI INSIDE OF AN E-PLANE SECTORAL HORN
REM   FOR LARGE VALUE OR RO1.
REM
REM   VARIABLE LIST:
REM
REM   WID       THE WIDTH OF THE HORN.
REM   RO1       THE AXIAL DISTANCE FROM THE APEX TO THE
REM             APERTURE.
REM   EPHI      THE MAXIMUM VALUE OF EPHI.
REM
10    CLEAR
20    INPUT"WIDTH OF HORN";WID
30    INPUT"RO1";RO1
40    PI=3.1415927
REM
50    EPHI=(SQR((2*PI)**2-(PI/WID)**2))*SQR(1/PI*PI*RO1)
REM
60    PRINT"EPHI=";EPHI
70    END
```

```
REM   THIS IS PROGRAM FIVE.  IT CALCULATES THE ABSOLUTE
REM   VALUE OF THE ELECTRIC FIELD AT A VALUE THETA, FOR
REM   A HORN WITH A FLARE ANGLE, FLANG.  THE ASYMPTOTIC
REM   VALUES OF THE HANKEL FUNCTIONS ARE USED TO APPROXI-
REM   MATE THE ELECTRIC FIELD FOR A LARGE RO1.
REM
REM   VARIABLE LIST:
REM
REM   RO1       THE DISTANCE FROM THE APEX TO THE APERTURE
REM             OF THE HORN.
REM   ARE       THE DISTANCE FROM THE APEX TO THE OBSERVAT-
REM             ION POINT.
REM   WID       THE WIDTH OF THE HORN.
REM   THETA     THE ANGLE IN DEGREES BETWEEN ARE AND THE
REM             AXIS IN THE CENTER OF THE APERTURE OF THE
REM             HORN.
REM   FLANG     THE FLARE ANGLE IN DEGREES
REM   FRAD      FLANG IN RADIANS.
REM   TRAD      THETA IN RADIANS.
REM   CNT       THE CONSTANT GIVEN BY CNT=((WID*SQR(RO1))
REM             /ARE).
REM   MAG       THE ABSOLUTE VALUE OF THE INTEGRAL VALUE.
REM   FIELD     THE MAXIMUM VALUE OF THE E-FIELD.
REM   REAL      THE REAL PART OF THE INTEGRAL.
REM   IMAG      THE IMAGINARY PART OF THE INTEGRAL.
```

```
REM
10    CLEAR
20    INPUT"RO1=";RO1
30    INPUT"ARE=";ARE
40    INPUT"WID=";WID
50    INPUT"FLARE ANGLE=";FLANG
REM
60    FOR THETA=0 TO 90  STEP 2
70    PI=3.1415927
80    FRAD=FLANG*PI/180
90    TRAD=THETA*PI/180
100   A=-FRAD/2
110   B=FRAD/2
120   GOSUB 5000
130   GOSUB 6000
140   CNT=((WID*SQR(RO1))/ARE)
150   MAG=SQR((REAL**2)+(IMAG**2))
160   FIELD=CNT*MAG*(1+COS(TRAD))
170   PRINT"EMAX(";FLANG")=;FIELD
180   NEXT THETA
190 END
```

```
5000  N=100
5010  W=(B-A)/N
5020  FOR I=0 TO N
5030  X=A+I*W
5040  F=(COS((180/FLANG)*X))*(COS((2*PI*R01)*COS(X-TRAD)))
5050  T=L/2-INT(L/2)
5060  IF T.GT.0 AND L.LT.N THEN LET P=4*F
5070  IF T.EQ.0 AND L.LT.(N-1) THEN LET P=2*F
5080  IF L.EQ.0 OR L.EQ.N THEN LET P=F
5090  L=L+1
5100  R=R+P
5110  NEXT I
5120  REAL=W*R/3
5130  RETURN
REM
REM
6000  N=100
6010  W=(B-A)/N
6020  FOR I=0 TO N
6030  X=A+I*W
6040  F=(COS((180/FLANG)*X))*(SIN((2*PI*R01)*COS(X-TRAD)))
6050  T=L/2-INT(L/2)
6060  IF T.GT.0 AND L.LT.N THEN LET P=4*F
```

```
6070  IF T.EQ.0 AND L.LT.(N-1) THEN LET P=2*F
6080  IF L.EQ.0 OR L.EQ.N THEN LET P=F
6090  L=L+1
6100  R=R+P
6110  NEXT I
6120  IMAG=W*R/3
6130  RETURN
```

VITA

Walter Lee Trammell was born in Jacksboro, Tennessee on January 4, 1955. He attended elementary and high school in Campbell County and graduated in June 1973. That September he entered Cumberland College in Williamsburg, Kentucky, and in June 1977 he received a Bachelor of Science in Mathematics. He was a teacher for three years and then returned to Cumberland College to prepare for medical school. During the preparation, he decided to attend The University of Tennessee, Knoxville and major in Electrical Engineering. After completing his Bachelor of Science in Electrical Engineering in May 1987, he began study toward a Master's degree in Electrical Engineering which was awarded in May 1989.

The author is now working on his Doctor of Philosophy degree in Electrical Engineering at The University of Alabama at Huntsville and is employed by the United States Army Strategic Defense Command in Huntsville, Alabama.